Assessment of water erosion in the Iguerferouane watershed (western High Atlas, Morocco) using the erosion potential model and geospatial tools

Khadija Oudour[1]*[iD], Ahmed Algouti[1], Abdellah Algouti[1], Mohamed Lakhlili[1],
Khadija Lamrani[1], Sabah Ben Elhamdi[1], Abdennacer El Myr[1],
Chaima Ben Tabet[1], Naji Jdaba[2][iD]

[1] Department of Geology, Geoscience Geotourism Natural Hazards and Remote Sensing Laboratory (2GRNT), Faculty of Sciences Semlalia, University of Cadi Ayyad, BP, 2390, 40000, Marrakesh, Morocco
[2] University of Ibn Zohr, Faculty of sciences, Laboratory of Geosciences, environment and Geomatics, Department of Geology, Agadir, Morocco
* Corresponding author's e-mail: k.oudour.ced@uca.ac.ma

ABSTRACT

The Iguerferouane watershed, located in the western High Atlas of Morocco, is highly vulnerable to soil erosion for its geomorphological and climatic characteristics. This process threatens the physical environment, agricultural productivity, and local socio-economic development. The present study aims to quantitatively assess soil erosion in this watershed and to map the spatial patterns of erosion risk, to achieve this, the erosion potential method (EPM) was applied by integrating multiple factors such as climate, slope, land cover, and soil type. Spatial datasets were processed using geographic information systems (GIS) to generate thematic layers, which were subsequently incorporated into the EPM framework to estimate both the magnitude and spatial variability of erosion. The results reveal significant spatial heterogeneity, with erosion rates ranging from 64 to 34,000 m³/km²/year and an annual mean soil loss of 5,312.36 m³/km². Severely affected areas, representing 33.76% of the watershed, are concentrated in the south, where steep slopes (40–267%), sparse vegetation, fragile lithology, and intense rainfall converge to accelerate erosion. Central and eastern sectors are moderately impacted, whereas northern areas experience limited erosion due to gentler topography and lower rainfall. These findings demonstrate that soil erosion in the Iguerferouane basin is driven primarily by the interaction topography, a degrading vegetation, rainfall aggressiveness, and lithological fragility. This study represents the first quantitative assessment of erosion in the iguerferouane watershed, providing insights into the spatial dynamics and main controlling factors of soil erosion in this area.

Keywords: water erosion, High-Atlas, Iguerferouane, watershed, erosion potential model.

INTRODUCTION

Soil loss due to erosion is a global phenomenon entailing severe negative impacts on ecosystems, societies, and livelihoods (Gourfi et al., 2024; Batunacun et al., 2019; Rafik et al., 2022). Anthropogenic, topographic, pedological, and climatic factors, especially water, play a decisive role in soil erosion. Indeed, rainfall and surface runoff are the main driving forces behind water erosion. (Deore and Pethkar, 2023). On a global scale, this phenomenon has quite the significant impact, affecting approximately 1.094 million hectares of arable land each year (Noor et al., 2013; El Mouatassime et al., 2019). Morocco, along the same line, is vulnerable to erosion in an increasing rate over the years (Aoufa et al., 2022).

Water erosion is the leading cause of land degradation in Morocco (Fartas et al., 2022), significantly affecting up to 40% of the national territory (FAO and ITPS, 2015) and threatening nearly 75% of cultivated lands (Messaoudi et al., 2024). For the past 30 years, Morocco has experienced one of the most severe drought episodes

in its contemporary history. Particularly, in the High Atlas region, vegetation growth is limited due to worsening water deficits (Nouaim et al., 2023), which negatively disturbing soil stability and increasing its vulnerability to water erosion. Moreover, ever-increasing human activities, such as urbanization and certain agricultural practices, exacerbate this vulnerability.

To assess and predict soil erosion, various approaches have been applied, including statistical, physical, and empirical models. Statistical methods such as the frequency ratio (FR) are widely used to analyze the factors influencing gully formation. These approaches enable individual assessment of each contributing factor (Fadil and El Wahidi, 2023) and enhance the understanding of erosion processes. Physical models, on the other hand, rely on mathematical equations to simulate erosion, transport, and sedimentation processes. While they provide detailed modeling of water flows and erosion dynamics, their application requires numerous parameters, which can limit their use in large-scale watershed studies (Raza et al., 2021).

Empirical models are therefore widely used in soil erosion modeling, as they demand minimal data, making them simple and flexible to apply. Some of the most commonly used empirical models are the universal soil loss equation (USLE; Wischmeier and Smith, 1978) and its variants MUSLE (Williams, 1975) and RUSLE (Renard et al., 1991), These models are extensively applied to estimate soil loss and identify the most vulnerable areas (Oudchaira et al., 2024; Khemiri and Jebari, 2021; Tian et al., 2021). However, since they were primarily developed for sheet and rill erosion, they are unable to simulate gully erosion or sediments deposition. In addition, their unsuitability for mountainous areas further limits their application in such contexts.

The model developed by Gavrilovic (1972), one of the empirical methods named erosion potential method (EPM), represents a valuable alternative, making it particularly suitable for mountainous watersheds. Its relatively low data requirements and adaptability to GIS environments further enhance its applicability. In Morocco, the model has been widely applied, for instance by Lakhili et al. (2021) in the Beht watershed, Ouallali et al. (2020) in the Arbaa Ayacha watershed, and Elbadaoui et al. (2023) in the Toudgha River watershed in the central High Atlas.

Located on the northern flank of the western High Atlas, the Iguerferouane watershed has not yet been examined in detail with respect to soil erosion and its controlling factors. While the Tensift basin, which includes Iguerferouane, has been the subject of several regional erosion studies (e.g., Meliho et al., 2020; Bamou et al., 2024), these remain broad in scope and lack detailed information at the sub-watershed scale. No quantitative assessment of erosion has been conducted specifically in the Iguerferouane watershed, despite the area being highly affected by water erosion and its communities relying heavily on agriculture. To address this gap, the study applies an integrated approach combining the EPM with GIS and remote sensing to analyze and map erosion processes. The objectives are to quantify soil loss, identify erosion-prone areas, determine the dominant controlling factors, and generate spatial information that may contribute to a better understanding of erosion processes and potentially inform future soil conservation and land management efforts.

Study area

The Iguerferouane watershed is situated in southwestern Morocco, approximately 30 km southeast of Marrakech, on the northern flank of the High Atlas Mountains. It extends between latitudes 31.322468°N and 31.549283°N, and longitudes 7.635334°W and 7.760439°W (Figure 1).

The study area is included within the larger Tensift basin and extends over a distance of 100 kilometers, covering a total area of 299.023 km². Elevation in the basin ranges from 522 m to 2731 m, with an average altitude of 1626.5 m. The topography is characterized by slopes varying from 0° to 66°, with an average slope of 51.01 m/km.

Geologically, the Iguerferouane catchment encompasses the northeastern slopes of the High Atlas Meso-Cenozoic mountain belt in its upstream section and extends into the foreland basin downstream (Figure 1c), and the stratigraphical records displays significant lithological diversity. In the upstream section of the Iguerferouabe watershed, the Upper Carboniferous Paleozoic basement consists of schist and marl facies, which is unconformably overlian by Triassic formations (Frizon de Lamotte et al., 2008). The Meso-Cenozoic cover comprises Triassic detrital and evaporitic deposits, overlain by late Triassic basalts and Lower Jurassic (Lias) carbonate formations. The Cretaceous sequence includes fossiliferous dolomites from
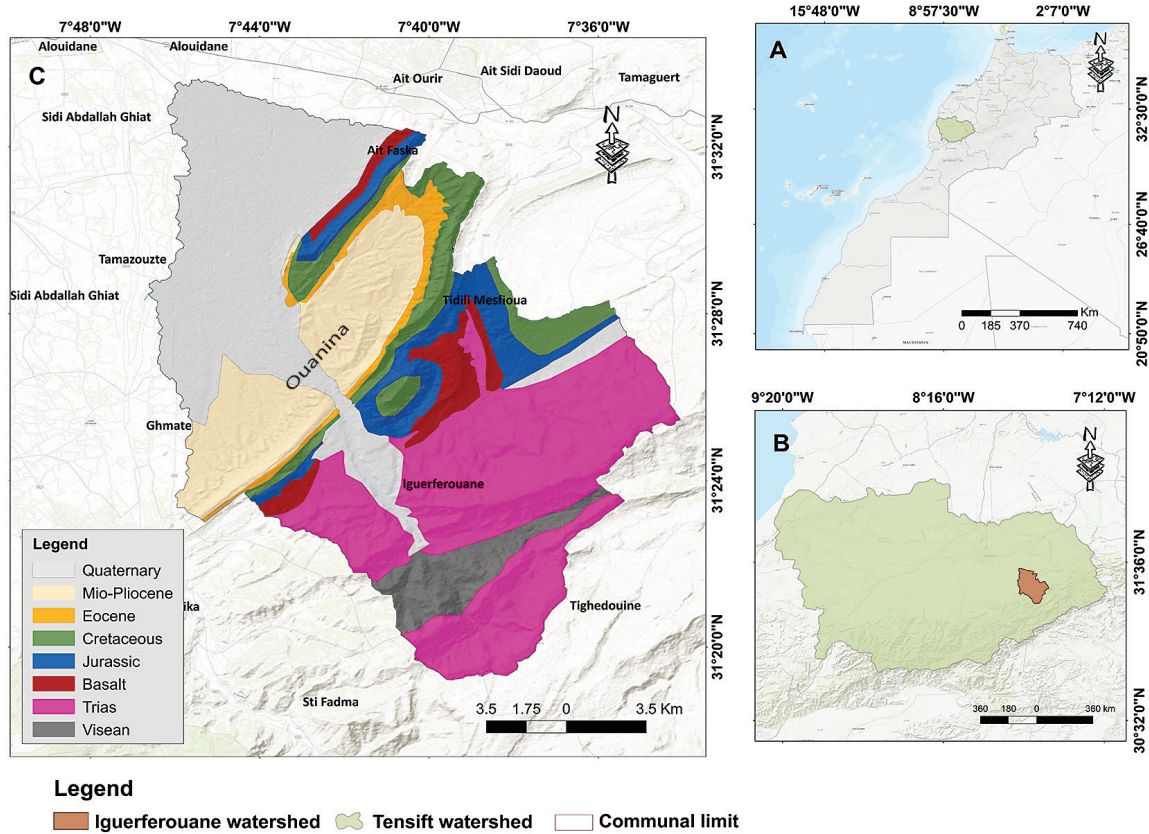
Figure 1. (a) Location of the study area in Morocco; (b) location of the study area within the Tensift watershed; (c) simplified geological map of the study area, based on the geological map of Morocco and the Aït Ourir Basin (1:200,000; 1:10,000)

the Aptian-Albian, as well as Senonian silt-stones and red sandstones. Within the Ouanina syncline, the Tertiary period is marked by flint-bearing limestones, phosphatic layers, and Oligo-Miocene conglomeratic deposits. Lastly, the Quaternary formations, composed of sandstone and conglomerates, reflect the ongoing erosion of the Atlas Mountains.

MATERIALS AND METHODS

To evaluate water erosion in the Iguerferouane watershed, we applied the erosion potential model. This model considers key factors influencing soil loss, such as slope, vegetation cover, soil and surface formations, and precipitation. A distinctive feature of this model is the inclusion of temperature as an additional factor in the assessment of water erosion (Chaouan Jamal, 2015).These variables are integrated within a GIS framework (i.e., Arcgis 10.8), where the EPM equation (Equation 1) is applied to generate a spatially explicit soil loss map.

$$W = T \times H \times \pi \times \sqrt{Z^3} \qquad (1)$$

where: W is total annual volume of detached soil (m³/km²./year), H is mean annual precipitation (mm), T is temperature coefficient, which is defined as (Gavrilovic, 1998):

$$T = \sqrt{t0/10 + 0.1} \qquad (2)$$

where: t_0 is Annual mean temperature (°C).

Additionaly, Z [-],the potential erosion coefficient, indicates the intensity of erosion processes in the watershed (Baiddah et al., 2025; Hssain, 2014) and is calculated as follows (Staut, 2004):

$$Z = Xa \times Y \times \phi \times \sqrt{Ja} \qquad (3)$$

where: X_a is soil protection coefficient, Y is Soil erosion sensitivity, φ = type and extent of erosion coefficient ($0.1 \leq \varphi \leq 1$) and J_a is slope coefficient (%).

The methodological workflow used to apply the EPM model for generating the soil loss map is presented in Figure 2, illustrating the successive steps of the process.
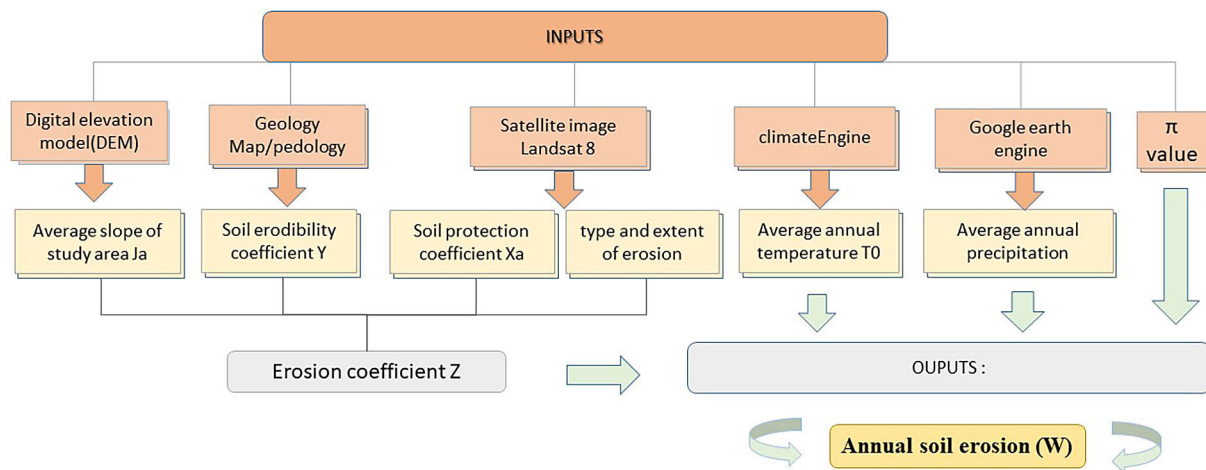
Figure 2. Flow chart of the adopted methodology of this research

Temperature coefficient T

Temperature influences soil erosion by affecting evapotranspiration rates and contributing to rock disintegration through thermal weathering (Coque, 1977; Oulghazi, 2023). Since no direct instrumental measurements were available in the watershed, mean annual temperature (t_0) was estimated using MODIS/Terra LST data accessed through the ClimateEngine platform (https://app. climateengine.org). The dataset, covering the period 2000–2023, was then used to calculate the temperature coefficient (T) according to Equation 2.

Precipitation index

Precipitation considered the most influential factor in water erosion, unlike other indices, precipitation in the Gavrilovic model is used in its raw form, expressed in millimeters, without any modification. The precipitation data used in this study were extracted from the Google Earth Engine platform (https://earthengine.google.com/), using the Climate Hazards Group InfraRed Precipitation with Station data (CHIRPS) product covering the period from 1981 to 2023.

Soil protection coefficient (Xa)

The soil protection coefficient (X_a) is related to vegetation cover, which enhances roughness and cohesion, improves soil stability, and consequently reduces erosivity and soil erosion (Rey et al., 2004; He et al., 2008; Asima et al., 2022).

In this study, the coefficient X_a was derived from the modified normalized difference vegetation index (XaNDVI), calculated from Landsat 8 OLI imagery (2023).The NDVI was computed in ArcGis 10.8 using Band 5(NIR) and Band 4 (Red) according to the formula NDVI = ((NIR-Red))/((NIR+Red)) The resulting values were then converted into Xa values using the equation 4 proposed by Chaouan Jamal (2015).

$$Xa = (XaNDVI - 0.61) \times (-1.25) \qquad (4)$$

where: *Xa* is Soil protection coefficient and *XaN-DVI* is the adjusted *NDVI* vegetation index.

Soil erosion sensitivity (Y)

Soil sensitivity to erosion refers to its vulnerability to detachment and transportation of particles (Wischmeier et al., 1971). It depends on several properties, including texture, organic matter content, structure, and permeability.

In this study, soil erosion sensitivity (Y) is determined using the Equation 5 developed by Wischmeier and Smith (1978):

$$K = \left(\begin{array}{c} (2.1 \times 10^{-4} \times M^{1.14}) \times (12 - a) + \\ + 3.25 \times (b - 2) + 2.5 \times (c - 3) \end{array} \right) / 100 \;(5)$$

where: M – (% silt + % fine sand) × (100 – % clay); a – Organic matter content (%) ; b – Permeability code ; c – Soil structure code.

To obtain these parameters, 25 soil samples were collected across the watershed (Figure 3, Figure 4.a,b). Grain size distribution was determined by laser granulometry (Figure 4c), and organic matter content was measured using the loss on ignition method (Figure 4d). Soil structure and permeability codes were subsequently assigned
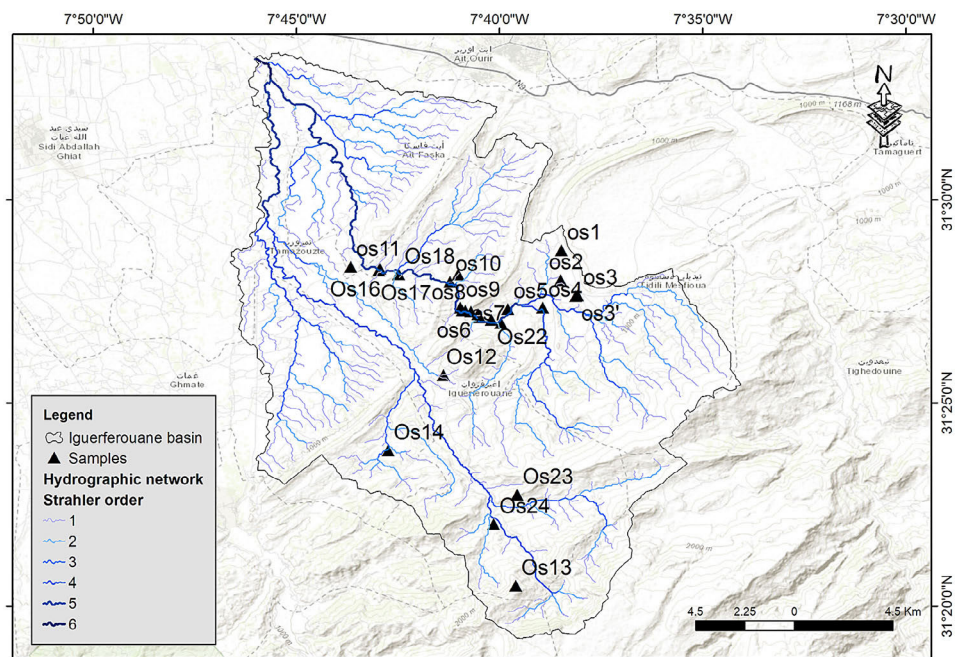
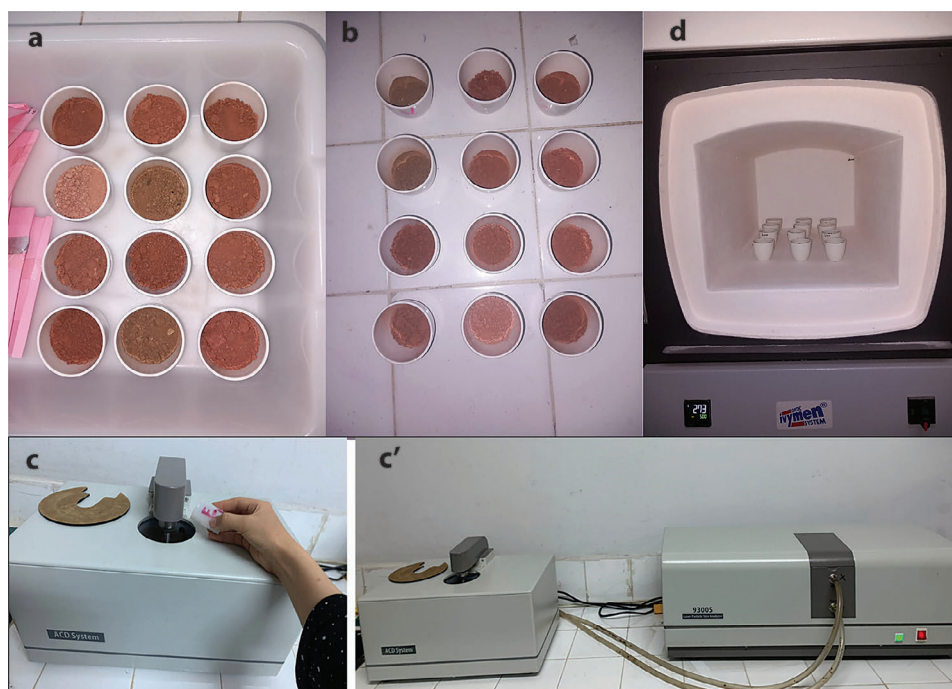**Figure 3.** Locations of soil sampling points

Figure 4. (a,b) soil samples; (c, c'): laser particle size analyzer BT-9300S; (d) Muffle furnace employed for the loss on ignition (LOI) analysis of soil samples

based on the proportions of sand, silt, and clay, by plotting the samples on soil texture diagrams.

Types and extent of erosion coefficient (φ)

This coefficient evaluates the current intensity of water erosion within the watershed and helps identify visible forms of erosion (e.g., streams, gullies, alluvial deposits). It is influenced by multiple factors such as lithology, vegetation, climate, topography, and land use. In this study, the φ coefficient was derived from Landsat 8 OLI satellite imagery using the following Equation 6 (Milevski et al., 2008):

Table 1. Type of soil erosion based on (φ) (Gavrilović 1988)

φ factor	Coefficient of type and extent of erosion φ
0.1–0.2	Slight erosion on the catchment
0.3–0.5	20–50% of the catchment area has erosion in rivers and streams
0.6–0.7	Erosion in rivers, gullies, and alluvial deposits, karstic erosion
0.8–0.9	50–80% of drainage basin is impacted by surface erosion and landslides
0.9–1.00	Erosion affects entire catchment

$$\varphi = \sqrt{(B4/Qmax)} \qquad (6)$$

where: $B4$ = Band 4 (Red) of the Landsat 8 OLI image and $Qmax$ is Maximum radiance value of the band 4 it is obtained from the attached MTL file of Landsat 8 images.

As indicated by Gavrilovic and Lazarevic (1985), the relationship between the calculated values and the severity of erosive processes is established using the reference table (Table 1).

Slope coefficient (Ja)

Slope is one of the most critical factors in soil erosion as steeper slopes lead to faster runoff and stronger erosive forces, thereby increasing soil loss (Wischmeier and Smith, 1978). The slope map of the Iguerferouane watershed was derived from the 30 m resolution ASTER Global Digital Elevation Model (ASTGTM) (https://cmr.earthdata.nasa.gov/search/concepts/C1711961296-LPCLOUD.html), using the spatial analyst tool in ArcGIS 10.8, which was employed to calculate the slope coefficient (Ja).

RESULTS

Temperature

The temperature index T of the studied watershed (Figure 5) ranged from 1.25 to 2. Lower values were recorded at higher altitudes within the study area, while higher values were observed at lower elevations of the watershed.

Precipitation index

The results of precipitation index (Figure 6) in the study area show precipitation intensity varying between 300 mm and 480 mm, with a gradient that increases both with elevation and from the downstream to the upstream parts of the watershed. This pattern influences and enhances erosion processes particularly in the upstream zones.
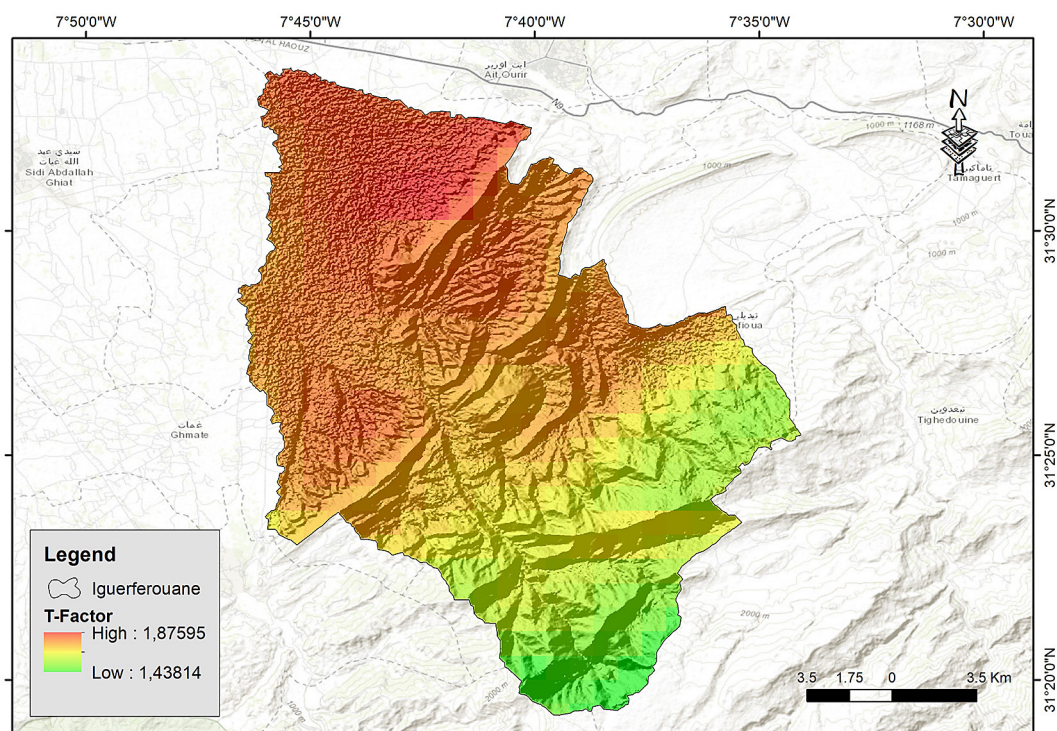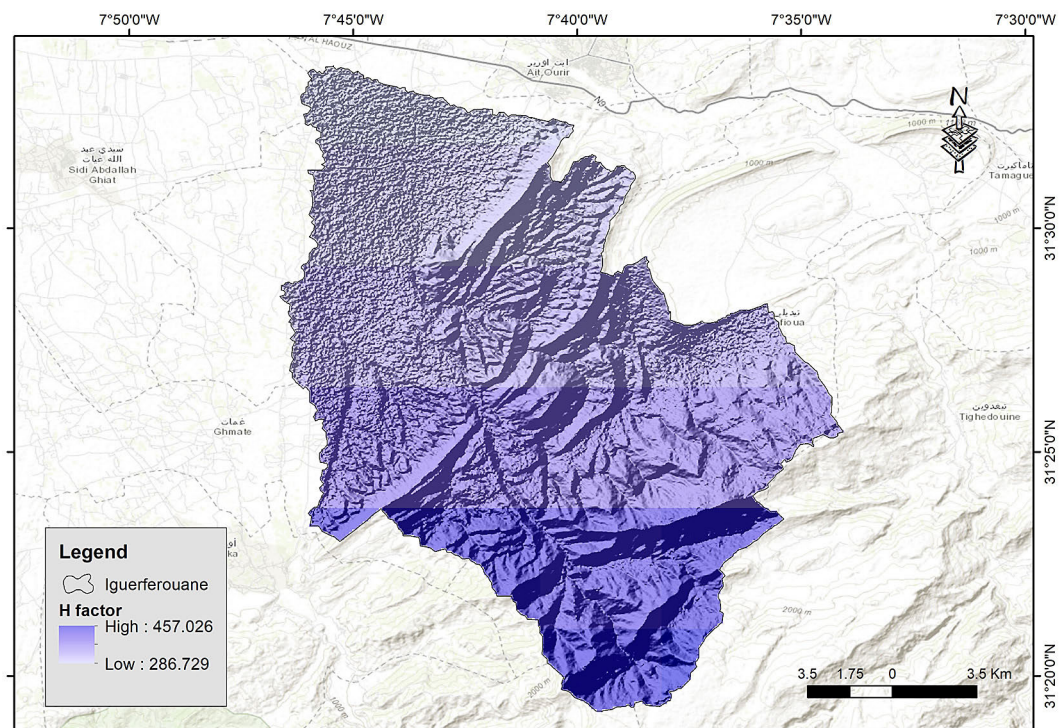

Figure 5. Map of temperature coefficient (T factor)

Figure 6. Rainfall map (H factor)

Soil erosion sensitivity (Y)

As mentioned, the computation of the soil sensitivity coefficient (Y) requires the parameters M, a, b, and c. These outcomes are summarized in Table 2 and illustrated in Figure 7, which show that most samples are classified as silt loam to silt. Organic matter is generally low (< 1.5%) with only a few samples reaching up to 2.8%. Structure and permeability codes are mainly between 3 and 4, reflecting weak structure and moderate to poor permeability.

The integration of these factors allowed calculation of the soil sensitivity coefficient (Y) and the production of a spatial map of soil sensitivity (Figure 8). The coefficient values range between 0.49 and 0.69, which indicates moderate to high soil sensitivity to erosion across the Iguerferouane basin.

Vegetation coefficient (Xa)

The vegetation coefficient results (Figure 9) indicate that areas lacking vegetation exhibit high protection coefficient values (Xa), reflecting insufficient soil protection. Conversely, vegetated zones display low Xa values, corresponding to better soil protection. Xa values in the study area range from 0.32 to 0.82, with the lowest values found in densely vegetated zones and the highest in unvegetated areas such as badlands. Following EPM guidelines (Zorgan, 1988), most of the study area falls within the 0.6–0.8 class, characterized by degraded pastures and cultivated lands. The next class, 0.4–0.6, includes damaged forests, shrubs, and some pastures, while the 0.32–0.4 class corresponds to natural forests and riparian vegetation. The analysis reveals that the majority of the Iguerferouane basin is sparsely and poorly vegetated, significantly reducing soil protection and thereby increasing susceptibility to erosion.

Erosion type and extent coefficient (φ)

The results regarding the type and extent of water erosion (Figure 10) indicate coefficient values between 0.35 and 0.59. According to this index, a very high erosion risk is found in the northern and northwestern parts of the basin, where vegetation is sparse or absent. In contrast, the southern sector, where vegetation cover is denser, shows lower erosion risk values.

Based on Gavrilović's classification (1988), the study area is mainly affected by two types of erosion: channel erosion, impacting 20–50% of the watershed, and gully and alluvial deposit erosion within streams and ravines.

Table 2. Results of soil analyses

Sample	Clay (%)	Silt (%)	Fine sand (%)	Organic matter (%)	Texture	S	P
OS1	12.25	76.98	10.77	2.78	Silt loam	3	3
OS2	11.96	81.51	6.53	2.40	Silt loam	4	4
OS3	9.12	84.57	6.31	0.82	Silt	4	4
OS3'	12.62	84.35	3.03	1.17	Silt loam	3	3
OS4	21.13	76.31	2.56	1.10	Silt loam	3	3
OS5	8.78	84.33	6.89	0.82	Silt	4	4
OS6	12.08	79.16	8.76	1.03	Silt loam	3	3
OS7	21.15	78.29	0.56	1.56	Silt loam	3	3
OS8	15.85	74.39	9.76	0.97	Silt loam	3	3
OS9	9.88	87.55	2.57	1.07	Silt	4	4
OS10	7.38	82.84	9.78	1.11	Silt	4	4
OS11	10.96	78.77	10.27	1.01	Silt loam	3	3
OS13	15.12	80.62	4.26	1.25	Silt loam	3	3
OS12	22.67	73.85	3.48	1.18	Silt loam	3	3
OS14	19.34	71.10	9.56	1.38	Silt loam	3	3
OS15	11.45	82.49	6.06	2.82	Silt	4	4
OS16	9.77	73.87	16.36	1.11	Silt loam	3	3
OS17	9.10	73.12	17.78	1.06	Silt loam	3	3
OS18	9.75	81.48	8.77	2.66	Silt	4	4
OS19	4.86	67.63	27.51	2.33	Silt loam	3	3
OS20	12.53	78.84	8.63	1.26	Silt loam	3	3
OS21	5.76	63.43	30.81	1.42	Silt loam	3	3
OS22	6.54	76.20	17.26	2.50	Silt loam	3	3
OS23	16.99	78.16	4.85	2.37	Silt loam	3	3
OS24	16.76	78.64	4.60	1.03	Silt loam	3	3
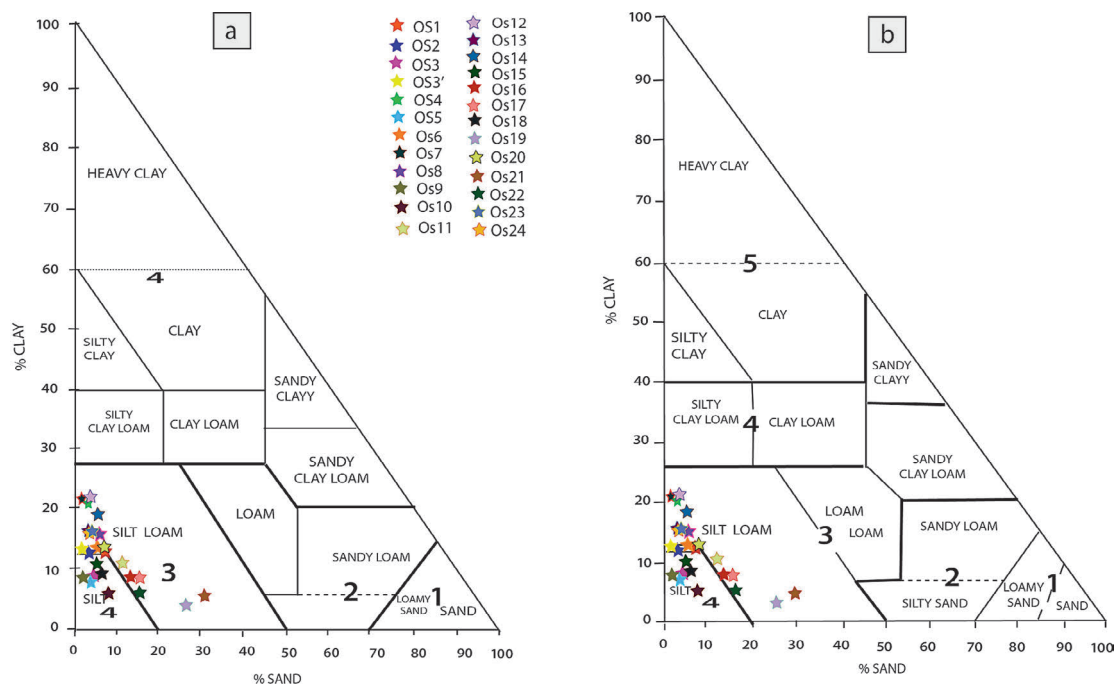
Figure 7. Triangular diagram based on texture classification indicating: (a) the code of permeability, (b) the code of structure
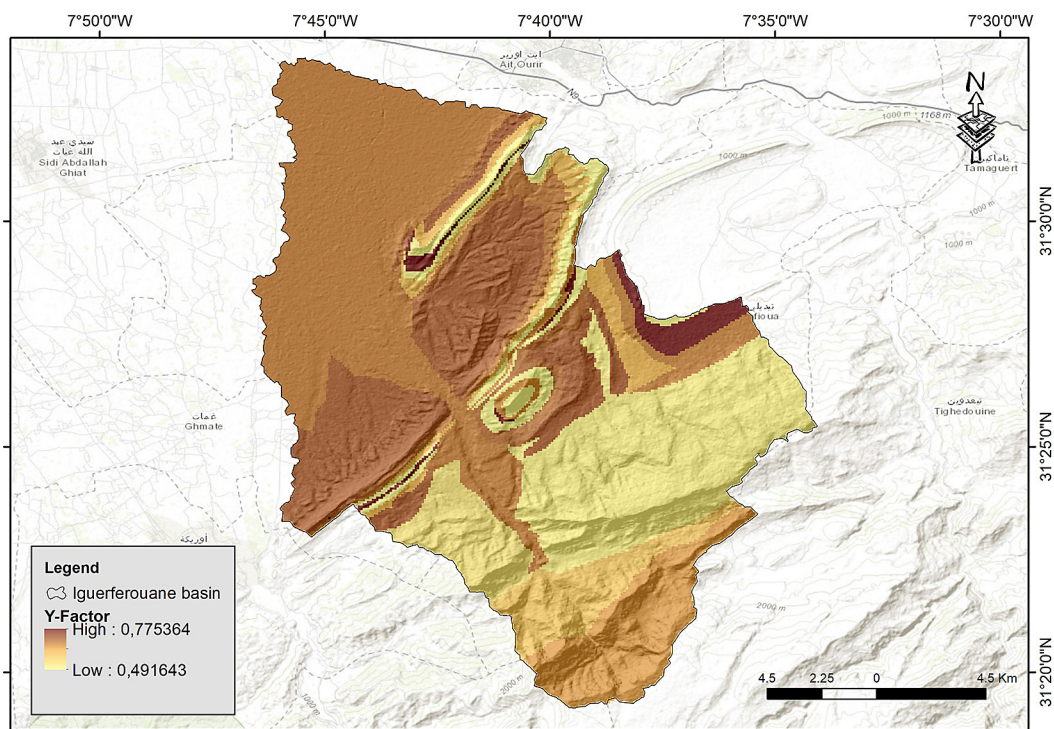
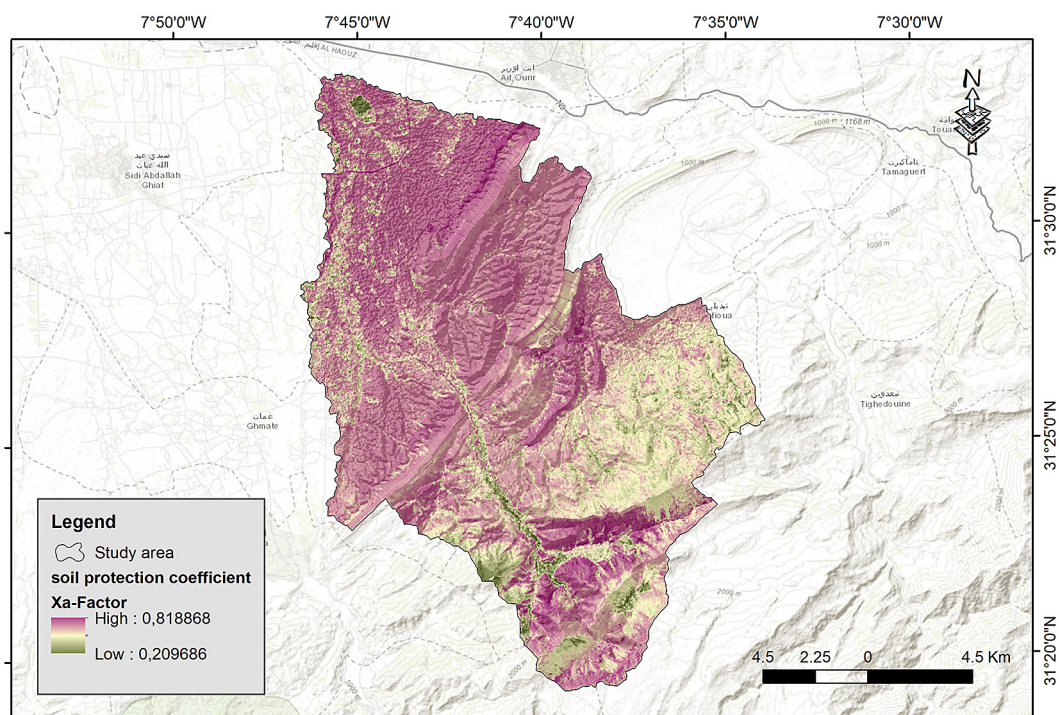**Figure 8.** Map of soil sensitivity coefficient (Y)

Figure 9. Map of the soil protection coefficient (Xa)

Slope (Ja)

Slopes within the Iguerferouane basin gradually change from upstream to downstream (Figure 11). Flat to moderate slopes (0–15%) dominate most of the basin, especially in the northern, eastern, and western areas. Intermediate slopes (15–40%) appear in transitional zones, reflecting more rugged terrain. Steep to very steep slopes (40–238%)
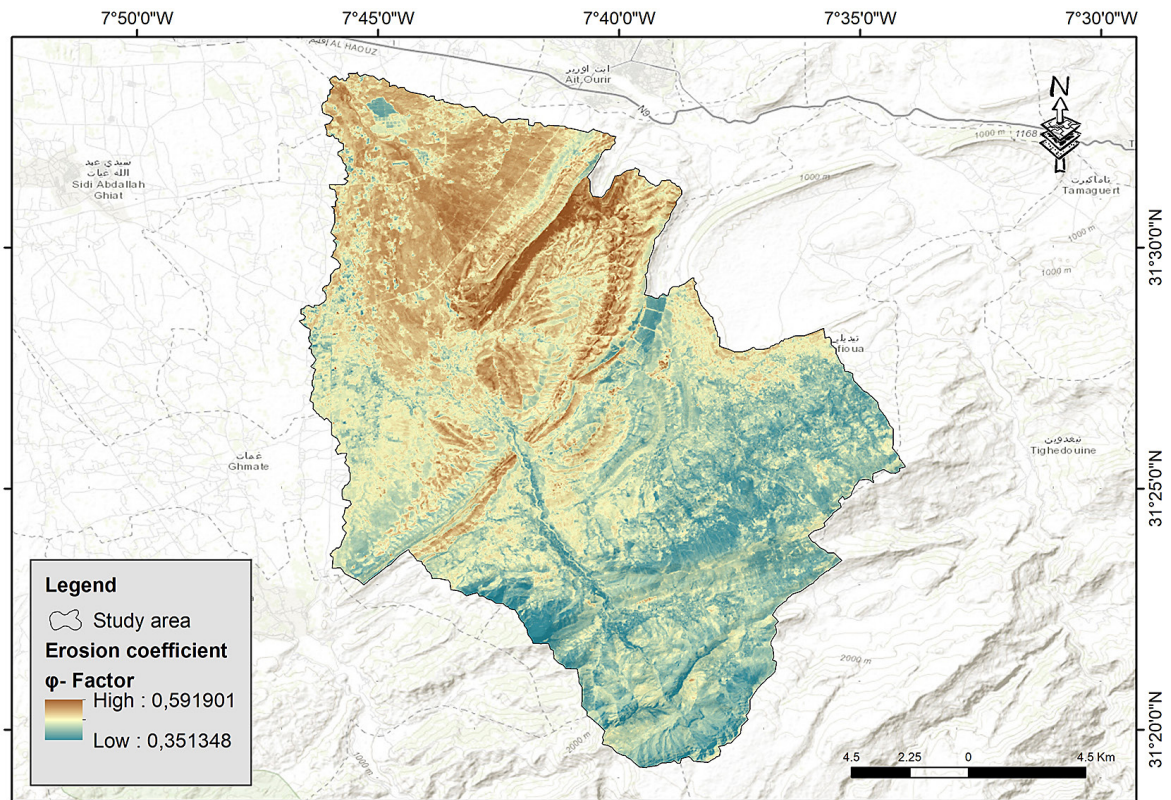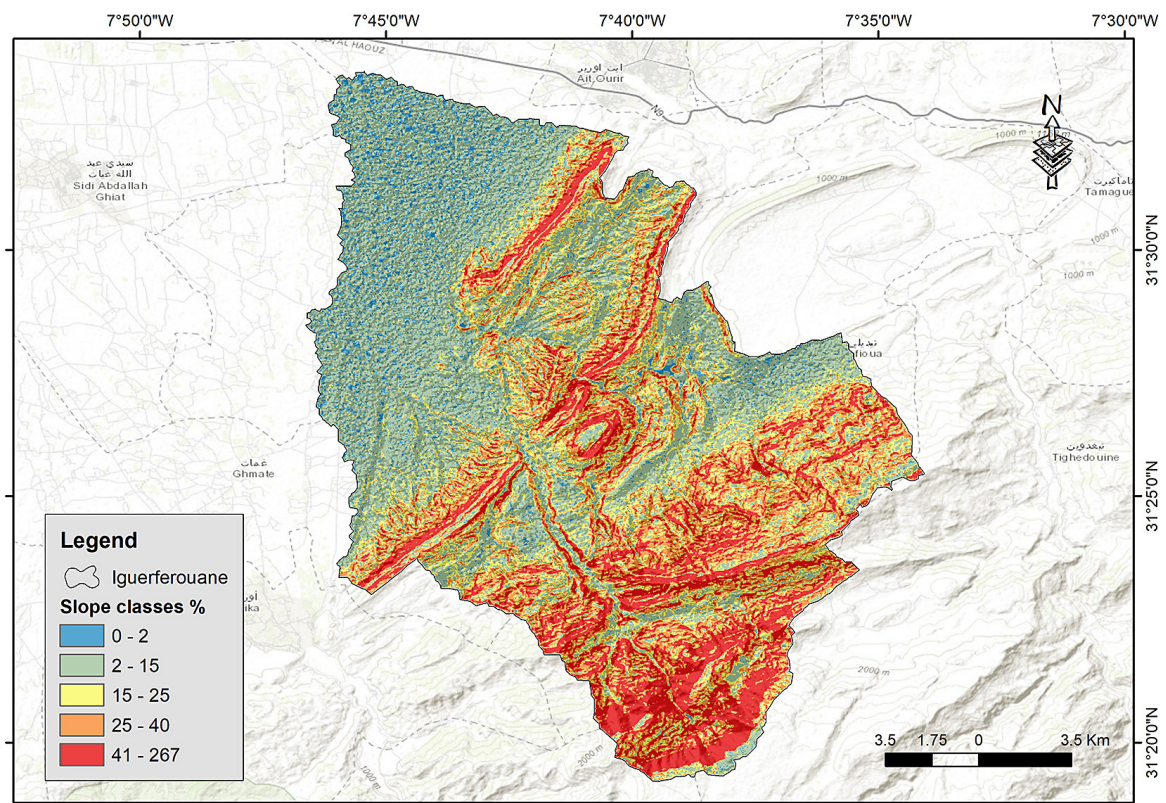
Figure 10. Map of type and extent of erosion coefficient

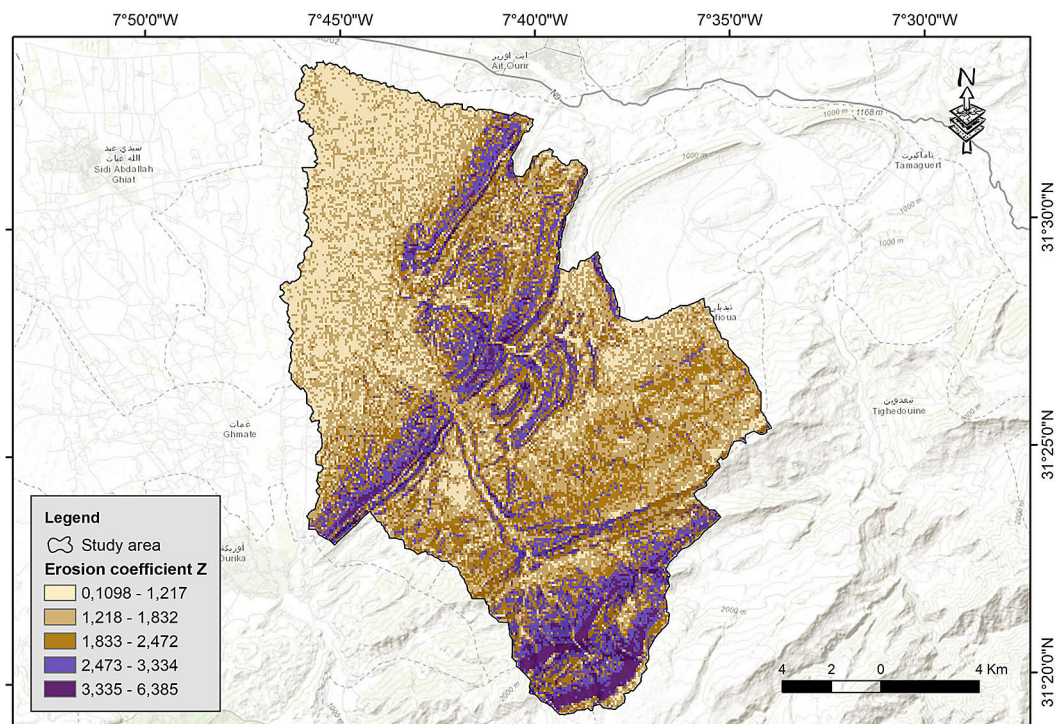**Figure 11.** Map of topographic coefficient (Ja)

Figure 12. Map of potential erosion coefficient (Z)

are concentrated in the central and southern parts of the basin, following mountain ridges and steep valleys.

Potential erosion coefficient (Z)

The erosion potential map (Z coefficient, Figure 12) was generated by combining data from the four main contributing factors: soil sensitivity to erosion, vegetation cover, current erosion patterns, and slope. The Z coefficient exhibits significant spatial variability. Areas with steep slopes, poor vegetation cover, highly erodible soils, and high erosion values correspond to the highest Z coefficients, indicating a very high erosion risk. In contrast, areas with good vegetation cover (low Xa), gentle slopes, and erosion resistant soils show low Z values, suggesting reduced erosion potential.

Annual soil erosion estimation (W)

The application of the EPM model enabled the generation of a quantitative map of water erosion (Figure 13) for the Iguerferouane watershed by integrating various erosion contributing factors. The estimated erosion rates range from 90 m³/km²/year to a maximum of 40,000 m³/km²/year. Significant water erosion is concentrated in the southernmost part of the basin (upstream) and

in the Ouanina depression. Conversely, the lowest erosion rates are found in the northern sector and the northeastern edge of the watershed.

DISCUSSION

The application of the EPM model has enabled both qualitative and quantitative assessment of soil loss in the Iguerferouane watershed. The results (Figure 13) show considerable variation, ranging from 64 to 34000 m³/km²/year, with an average estimated loss of 5,312.36 m³/km²/year.

Analysis of the annual erosion map (m³/km²/year) reveals a heterogeneous spatial distribution of soil loss. The most severely affected areas, covering 33.76% of the watershed, are primarily located in the southern part of the basin, with some extension toward central zones. The intensity of erosion in these regions is closely linked to the presence of steep slopes (40–267%) and high Xa values (0.81), indicating sparse or absent vegetation cover. This lack of vegetative protection exposes soils to the direct impact of rainfall, thereby promoting erosive processes.

Moreover, the heavier rainfall observed in the southern part of the basin (Figure 6) constitutes a major driver of runoff and sediment transport. Soils in these areas, predominantly sandy-loamy
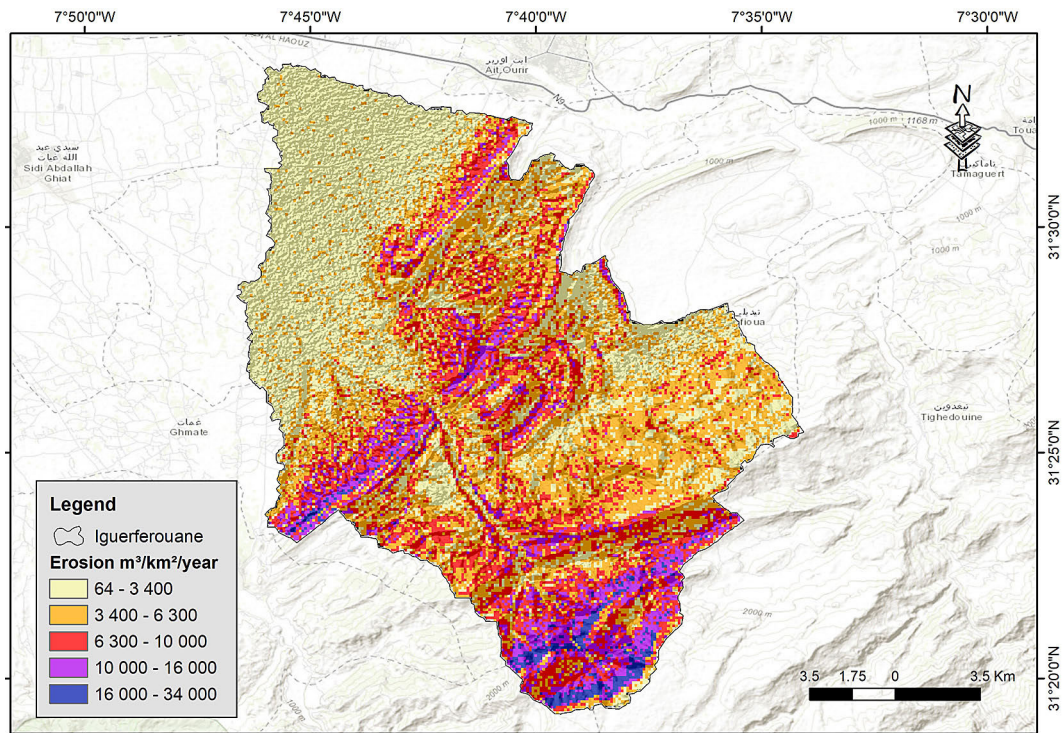
150

Figure 13. Map of annual soil loss in the Iguerferouane watershed

and low in organic matter, exhibit weak cohesion and are more prone to disintegration under the impact of precipitation, as indicated by the Y coefficient (0.51–0.65). However, the high vulnerability of these soils cannot be dissociated from their lithological context. The region is characterized by geological formations dominated by schists, marls, sandstones, and siltstones, which are often friable, weathered, and poorly consolidated factors that could have further enhanced susceptibility to erosion.

Moderately eroded areas, covering 22.51% of the basin, are mainly located in the central and eastern parts, surrounding the highly eroded zones. These areas are distinguished by gentler slopes and denser vegetation cover, which contribute to reduced erosion.

The least affected zones, accounting for 43.73% of the watershed, are situated in the northern part of Iguerferouane watershed. Although generally lacking vegetation, these regions experience limited erosion due to lower rainfall and a relatively gentle topography, particularly in the downstream sections. This configuration favors sediment accumulation, as evidenced by the Quaternary and Pliocene geological formations. These deposits, visible on the geological map (Figure 1c), illustrate the progressive accumulation of material over time and highlight the decisive role of topography in erosion and sedimentation processes.

Analysis of the temperature coefficient T, which increases from upstream to downstream, reflects the influence of altitude on temperature: higher elevations experience lower temperatures, while temperatures increase as elevation decreases toward the basin outlet. The examination of this coefficient (Figure 5) provides further insights into the erosion mechanisms in the region. An interesting observation is that although T is significantly higher in the lower part of the basin, erosion remains very limited there. This trend suggests that temperature alone has no direct impact on soil degradation unless it is coupled with steep slopes that enhance runoff and water erosion.

Overall, the findings indicate that the most severe soil degradation is primarily driven by a combination of factors accelerating erosion, especially the absence of vegetation cover. This conclusion is supported by several previous studies conducted in neighboring catchments, such as the Zat basin (Bouaida et al., 2023), and the Ourika basin (Ayt Ougougdal et al., 2020) localed to the east and the west of the studied area, respectively. Both studies confirm that erosion in these regions is mainly associated with climatic aggressiveness, rugged topography (steep slopes), sparse
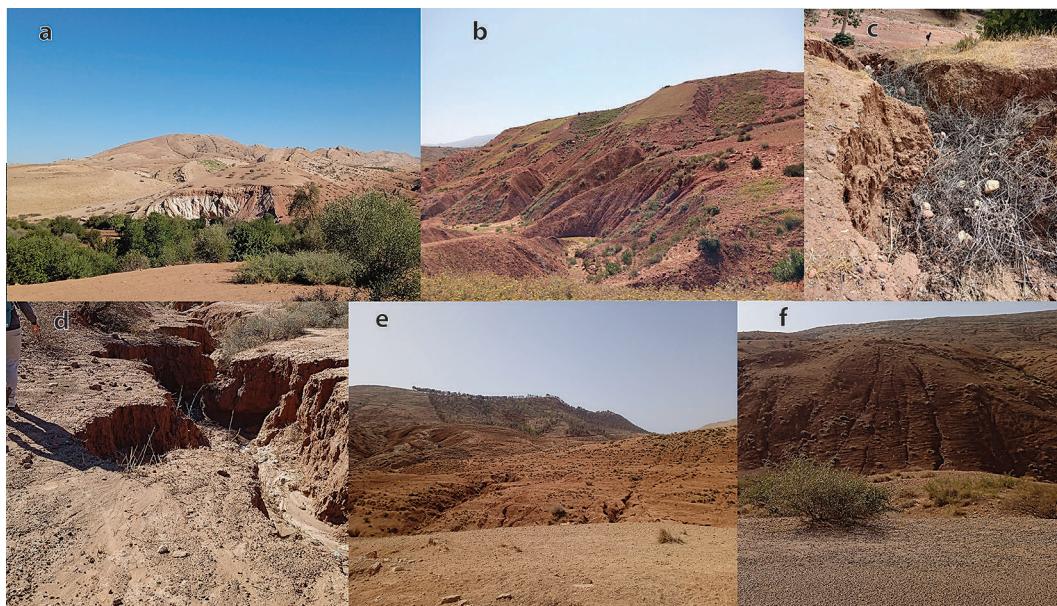
Figure 14. Field photographs of the Iguerferouane watershed: (a) gully erosion, (b) rill and gully erosion, (c) incipient gully formation, (d) advanced gully incision, (e) gully network development on degraded slopes, and (f) combined sheet and rill erosion on exposed hillslopes

vegetation, and the friable nature of the soils. These observations are also corroborated by Ziadi et al. (2023), who, using the PAP/RAC approach to model water erosion in the Tassaoute watershed (Central High Atlas), demonstrated that the most exposed areas are those combining loose terrain, steep slopes, and limited vegetation cover.

All the forementiened studies highlight the difficulty of attributing water erosion to a single factor. The results obtained in the Iguerferouane basin are consistent with this understanding, showing that erosion is particularly severe in areas with steep slopes, friable soils, degraded vegetation, and high precipitation. These findings are further supported by field evidence, where erosion features such as rills, gullies, and sediment deposits were observed in the most vulnerable parts of the basin (Figure 14). This confirms the relevance of the EPM model applied here to enhanced about undertating of soil erosion and its driving mechanism in the Iguererouane watershed.

CONCLUSION

This study aimed to assess water erosion in the Iguerferouane watershed through an integrated approach combining field and laboratory analyses with GIS and remote sensing techniques. The obtained results show that water erosion is influenced by a combination of climatic, topographical, and lithological factors. The lack of vegetation cover and steep slopes are key elements of soil degradation, particularly in the southern areas of the basin, where rainfall is higher. This study confirms that erosion in this region is mainly caused by a complex interaction between topography, vegetation, and geological characteristics. The EPM model is relevant for modeling this erosion and provides a better understanding of soil degradation dynamics at a regional scale. Appropriate soil management and adapted conservation strategies are necessary to mitigate the effects of erosion and preserve soil quality in this basin.

REFERENCES

1. Aoufa, M., Baghda, B., El Hadi, H., Chakiri, S., Hamoud, A., Zoraa, N., Zerdeb, M. A., Moussa, K. (2022). Quantification and evaluation of water erosion by RUSLE/GIS approach in the Ykem watershed (Western Morocco). *Ecological Engineering & Environmental Technology, 23*(5), 42–53. https://doi.org/10.12912/27197050/151631

2. Asima, H., Niedzinski, V., O'Donnell, F. C., Montgomery, J. (2022). Comparison of vegetation types for prevention of erosion and shallow slope failure on steep slopes in the southeastern USA. *Land, 11*(10), 1739. https://doi.org/10.3390/land11101739

3. Ayt Ougougdal, H., Yacoubi Khebiza, M., Messouli, M., Bounoua, L., Karmaoui, A. (2020). Delineation of vulnerable areas to water erosion in a mountain region using SDR-InVEST model: A case study of the Ourika watershed, Morocco. *Scientific African*, 10, e00646. https://doi.org/10.1016/j.sciaf.2020.e00646

4. Baiddah, A., Krimissa, S., Namous, M., Eloudi, H., Ismaili, M., Hajji, S., Aboutaib, F., Badreldin, N. (2025). Estimating erosion, sediment yield, and dam lifetime using revised universal soil loss equation and potential erosion model in the Chichaoua watershed and Boulaouane Dam, High Atlas, Morocco. *Ecological Engineering & Environmental Technology, 26*(3), 132–158. https://doi.org/10.12912/27197050/199824

5. Batunacun, W. R., Lakes, T., Yunfeng, H., Nendel, C. (2019). Identifying drivers of land degradation in Xilingol, China, between 1975 and 2015. *Land Use Policy, 83*, 543–559. https://doi.org/10.1016/j.landu sepol.2019.02.013

6. Bammou, Y., Benzougagh, B., Igmoullan, B., Kader, S., Ouallali, A., Spalevic, V., Sestras, P., Kuriqi, A. (2024). Spatial mapping for multi-hazard land management in sparsely vegetated watersheds using machine learning algorithms. *Environmental Earth Sciences, 83*, 447. https://doi.org/10.1007/s12665-024-11741-9

7. Bouaida, J., Witam, O., Ibnoussina, M. (2023). *Interest of Remote Sensing and GIS in the Study of Water Erosion: Case of the Zat Watershed (High Atlas, Morocco)*. In: Ben Ahmed, M. et al. (Eds.) Innovations in Smart Cities Applications 6. Springer. https://doi.org/10.1007/978-3-031-26852-6_58

8. Chaouan, J. (2015). *Mapping water erosion using remote sensing and GIS: Application of the EPM model in the Inaouen watershed (Middle Atlas, Morocco)* (Doctoral dissertation, FST Fès).

9. Combes, F., Hurand, A., Meunier, M. (1995). *The mountain forest: A remedy for floods* (Research Report No. 3, BVRE of Draix, Cemagref Publishing, Grenoble, France), 113–121.

10. Coque, R. (1977). *Geomorphology [Géomorphologie]*. Paris, France: A. Colin. (Collection U), 430.

11. Deore, S. J., Pethkar, S. S. (2023). *Evaluation of spatial and temporal variability in rainfall erosivity and soil erosion risk in Maharashtra, India*. In *Water, land, and forest susceptibility and sustainability: Geospatial approaches and modeling* 1, 353–379. Elsevier. https://doi.org/10.1016/B978-0-323-91880-0.00034-9

12. El Mouatassime, S., Boukdir, A., Karaoui, I., Skataric, G., Nacka, M., Khaledi Darvishan, A., Sestras, P., Spalevic, V. (2019). Modelling of soil erosion processes and runoff for sustainable watershed management: Case study Oued El Abid watershed, Morocco. *Agriculture & Forestry, 65*(4), 241–250. https://doi.org/10.17707/AgricultForest.65.4.22

13. Elbadaoui, H., Chikhaoui, M., Chehbouni, A., Loudyi, D. (2023). Evaluation of water erosion using the EPM model and remote sensing in the Toudgha watershed (Central High Atlas, Morocco) (in French). *European Scientific Journal (ESJ), 19*(2), 48–68. https://doi.org/10.19044/esj.2023.v19n2p48

14. Fadil, A., El Wahidi, F. (2023). Vers une nouvelle classification des modèles d'évaluation et de prédiction de l'érosion hydrique. *Physio-Géo, 19*, 83–112. https://doi.org/10.4000/physio-geo.15783

15. FAO & ITPS. 2015. *Status of the World's Soil Resources (SWSR). Food and Agriculture Organization of the United Nations and Intergovernmental Technical Panel on Soils, Rome, Italy*. In press.

16. Fartas, N., El Fellah, B., Mastere, M., Benzougagh, B., El Brahimi, M. (2022). Potential soil erosion modeled with RUSLE approach and geospatial techniques (GIS tools and remote sensing) in Oued Joumouaa watershed (Western Prerif-Morocco). *The Iraqi Geological Journal*, 47–61.

17. Frizon de Lamotte, D., Michard, A., Saddiqi, O., Chalouan, A., Lamotte, D. F. (2008). *The Atlas System*. In A. Michard, O. Saddiqi, A. Chalouan, D. Frizon de Lamotte (Eds.), *Continental evolution: The geology of Morocco*. Lecture Notes in Earth Sciences, 116, 133–202. Springer. https://doi.org/10.1007/978-3-540-77076-3_4

18. Gavrilović, S. (1972). Engineering of torrents and erosion. *Journal of Construction* (Special Issue), Belgrade, Yugoslavia.

19. Gavrilovic Z.Stefanovic M. (1998). *Methodology for identification and proclamation erosion zones. –Institute for development of Water Resources "Jaroslav Černi" – Belgrade*.

20. Gavrilovic, Z. (1988). Use of an empirical method erosion potential method for calcu-lating sediment production and transportation in unstudied or torrential streams. *International Conference on River Regime. Hydraulics Research Limited, Walling-ford,*

Oxon UK. 411–422.

21. Gourfi, A., Daoudi, L., Daoud, N. B., Fagel, N. (2024). Clay minerals in soils and sediment as tracers of provenance: The case study of the N'fis watershed, Morocco. *Soil Use and Management, 40*(1), e12925.

22. Hssaine, A.A. (2014). Elements on the hydrology of the Atlantic part of the Oud Guir (South-Eastern Morocco) and on the catastrophic flood of 10 October 2008. Physio-Geo. *Physical Geography and Environment, 8*, 337–354.

23. He, J. J., Cai, Q. G., Tang, Z. J. (2008). Wind tunnel experimental study on the effect of PAM on soil wind erosion control. *Environmental Monitoring and Assessment, 145*(1–3), 185–193.

24. Khemiri, S., Jebari, S. (2021). Application of the RUSLE model in the assessment of water erosion in Tunisia: Case of the Oued Erroumi watershed (in French). *Revue des Régions Arides*, *54*(2), 145–157.

25. Lakhili, F., Chaaouan, J., Qadem, Z., Benabdelhadi, M., Lahrach, A. (2021). GIS-based soil erosion estimation using the EPM method in the Beht watershed [Estimation de l'érosion des sols basée sur le SIG à l'aide de la méthode EPM dans le bassin versant de Beht]. *Environmental and Water Sciences, Public Health and Territorial Intelligence Journal, 5*(2), 588–59

26. Lavabre, J., Andréassian, V. (2000). *The forest: A tool for water management?* (in French) (*Mediterranean Forest, XXI*(2), 146–153).

27. Lazarevic R. The new method for erosion coefficient determination – Z. *Erosion – professional factsheet, 13*; 54–61. (In Serbian).

28. Messaoudi, B., Kabiri, L., Ait Lahssaine, I., Essafraoui, B., Kassou, A., El Ouali, M., Kadiri, A., Achbarou, Z., Ouali, L. (2024). Modeling water erosion vulnerability and identifying control measures in the Upper Guir watershed, Southeastern Morocco, through spatial analysis with GIS and MCDM. *Euro-Mediterranean Journal for Environmental Integration*. https://doi.org/10.1007/s41207-024-00551-x

29. Meliho, M., Khattabi, A., Mhammdi, N. (2020). Spatial assessment of soil erosion risk by integrating remote sensing and GIS techniques: A case of Tensift watershed in Morocco. *Environmental Earth Sciences, 79*(10). https://doi.org/10.1007/s12665-020-08955-y

30. Milevski, I., Blinkov, I., Trendafilov, A. (2008). Soil erosion processes and modelling in the upper Bregalnica catchment. Paper presented at the the *conference of the Danubial countries on the hydrological forecasting and hydrological bases of water management (XXIV), Bled, Slovenia*.

31. Mosaid, H., Barakat, A., Bustillo, V., Rais, J. (2022). Modeling and mapping of soil water erosion risks in the Srou basin (Middle Atlas, Morocco) using the EPM model, GIS, and magnetic susceptibility. *Journal of Landscape Ecology, 15*(1). https://doi.org/10.2478/jlecol-2022-0007

32. Noor, H., Fazli, S., Alibakhshi, S. M. (2013). Evaluation of the relationships between runoff-rainfall-sediment related nutrient loss (A case study: Kojour Watershed, Iran). *Soil Water Res, 8*, 172–177.

33. Nouaim, W., Rambourg, D., El Harti, A., Abderrahim, E., Merzouki, M., Karaoui, I. (2023). The estimation of water erosion with RUSLE and deposition model: A case study of the Bin El-Ouidane dam catchment area (High Atlas, Morocco). *Journal of Water and Land Development, 58*(VII–IX), 136–147. https://doi.org/10.24425/jwld.2023.146606

34. Ouallali, A., Aassoumi, H., Moukhchane, M., Moumou, A., Houssni, M., Spalevic, V., Keesstra, S. (2020). Sediment mobilization study on Cretaceous, Tertiary and Quaternary lithological formations of an external Rif catchment, Morocco. *Hydrological Sciences Journal, 65*(9), 1568–1582. https://doi.org/10.1080/02626667.2020.1755435

35. Oudchaira, A., Ziyadi, M., Barakat, A. (2024). Cartographie de l'érosion hydrique et des zones à risques à l'aide du modèle RUSLE et du SIG: Cas du bassin versant de l'Ichach, Moyen Atlas, Maroc. *Revue Marocaine des Sciences Agronomiques et Vétérinaires*.

36. Oulghazi, A. (2023). Assessment and mapping of the risk of water erosion in the watershed of the oued Issen using GIS and the empirical model EPM (Western High Atlas - Morocco). *Environmental and Water Sciences, Public Health & Territorial Intelligence, 7*(2), 986–995.

37. Rafik, A., Ibouh, H., El Fels, A. E. A., Eddahby, L., Mezzane, D., Bousfoul, M., Amazirh, A., Ouhamdouch, S., Bahir, M., Gourfi, A., Dhiba, D., Chehbouni, A. (2022). Soil salinity detection and mapping in an environment under water stress between 1984 and 2018 (case of the largest oasis in Africa-Morocco). *Remote Sensing, 14*(7), 1606. https://doi.org/10.3390/rs14071606

38. Raza, A., Ahrends, H., Habib-Ur-Rahman, M., Gaiser, T. (2021). Modeling approaches to assess soil erosion by water at the field scale with special emphasis on heterogeneity of soils and crops. *Land, 10*(4), 422. https://doi.org/10.3390/land10040422

39. Renard, K. G., Foster, G. R., Weesies, G. A., Porter, J. P. (1991). RUSLE: revised universal soil loss equation. *Journal of Soil and Water Conservation, 46*(1), 30–33.

40. Rey, F., Ballais, J.-L., Marre, A., Rovera, G. (2004). Role of vegetation in protection against surface water erosion (in French). *Proceedings of the French Academy of Sciences. Geoscience, 336*(11), 991–998. https://doi.org/10.1016/j.crte.2004.03.012

41. Staut, M., 2004. Recent erosional processes in the catchment of the Dragonja river, Unpublished graduate thesis. *Faculty of Arts, University of Ljubljana, Ljubljana* (in Serbian).

42. Tian, Y., Xie, H., Zhang, Y., Li, Y., Li, Z. (2021). Simulation and prediction of soil erosion processes in a typical watershed using RUSLE and GIS. *Water, 13*(2), 158.

43. Williams, J. R. (1975). *Sediment-yield prediction with universal equation using runoff energy factor.* In: Present and Prospective Technology for Predicting Sediment Yield and Sources. USDA.

44. Wischmeier, W. H., Johnson, C. B., Cross, B. V. (1971). A soil erodibility nomograph for farmland and construction sites. *Journal of Soil and Water Conservation, 26*.

45. Wischmeier, W.H., Smith, D.D. (1978). *Predicting rainfall erosion losses. A Guide to conservation planning.* United States Department of Agriculture, Agricultural Research Service (USDA-ARS) Handbook No. 537. United States Government Printing Office, Washington, DC.

46. Ziadi, K., Barakat, A., El Aloui, A., Ouayah, M., Namous, M. (2023). Modelling and mapping of soil erosion risk based on GIS and PAP/RAC guidelines in the watershed of Tassaoute (Central High-Atlas, Morocco). *Bulletin of Geography. Physical Geography Series,* (24), 65–83.

47. Zorgan, G. The use of an Empirical Method (Erosion Potential Method) for Calculating Sediment Production and Transportation in Unstudied or Torrential Stream. In: Proceeding of International Conference on River Regimen; Hydraulics Research Limited:Wallingford, Oxon, UK, 1988.